Global NEST Journal, Vol 25, No 2, pp 50-56

Synergistic removal of 1-(4-hydroxy-3-methoxyphenyl) ethenone (Apocynin) with enhanced immobilized and suspended Sr-doped $LaNiO_3$ based photo-catalytic membrane reactor under gamma irradiation

Ragunath S.[1], Srinivasa Rao Y.[2], Sujatha S.[3], and Gokulan R.[4]*
[1]Department of Civil Engineering, Jansons Institute of Technology, Coimbatore, Tamil Nadu - 641-659, India
[2]Department of Mechanical Engineering, Sri Sivani College of Engineering, Srikakulam, Andhra Pradesh, India
[3]Department of Civil Engineering, K. Ramakrishnan College of Technology, Trichy, Tamil Nadu - 621 112, India
[4]Department of Civil Engineering, GMR Institute of Technology, Rajam, Srikakulam, Andhra Pradesh – 532 127, India
Received: 07/10/2022, Accepted: 07/11/2022, Available online: 09/11/2022
*to whom all correspondence should be addressed: e-mail: gokulan.r@gmrit.edu
https://doi.org/10.30955/gnj.004508

Graphical abstract

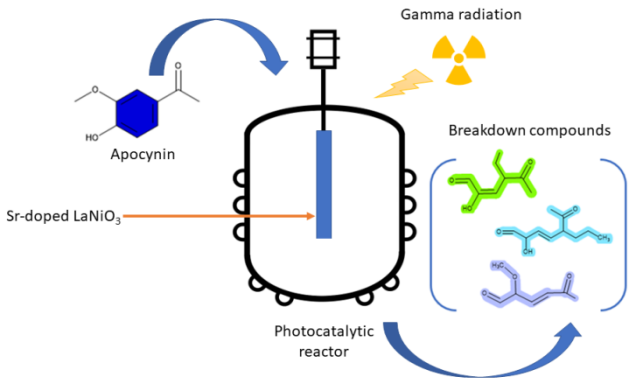

Abstract

The electrolytic approach was combined with radiolysis employing gamma radiation as an enhanced oxidation process to study the decomposition of 1-(4-Hydroxy-3-Methoxyphenyl) ethenone (Apocynin (ACN)). For Apocynin breakdown from effluent water, a photo-catalytic membrane reactor (PMR) was utilized with suspended and immobilised Sr-$LaNiO_3$ with regarding to gamma irradiation. For phase procedures, the impacts of basic Sr-$LaNiO_3$ on the PMR containing residual Sr-$LaNiO_3$ was investigated. An RO (Reverse Osmosis) membrane was integrated by way of the PMR under continuous circumstances to improve standard of water. At such a moderate Sr-$LaNiO_3$ dosage (0.8 g/L), ACN deterioration by the PMR with attached and immobilised Pt-$LaNiO_3$ was similar in both methods, but improved with larger Sr-$LaNiO_3$ doses for the reactor with coupled Pt-$LaNiO_3$.

Keywords: Apocynin, electrochemical degradation, photocatalytic reactor, gamma irradiation

1. Introduction

Several commodity-based industries that manufactures cork, pulp and paper uses a lot of electricity and freshwater, consequently, generates large volumes of sewage water. The generated sewage water contains effective levels of biochemical oxygen demand (BOD) and chemical oxygen demand (COD), intense colour, particulates, and non-biodegradable chemicals (Sevimli, 2005; Madureira *et al.*, 2014). The release of such unprocessed effluents might have a harmful influence on the environment because of the existence of these resistive chemicals, which should be reduced. Apocynin (ACN), a lignin degradation by-product found in pulp, paper and cork effluents. Microfiltration was used to remove apocynin from an aqueous mixture Gallic acid and Esculetin, according to some early research that were published (Acero *et al.*, 2005). The persistence effectiveness of the membrane was shown to be dependent on the nature of the membrane, with poor persistence for ACN in the utilized membranes. Hence, it is essential to eliminate ACN from water prior to release into freshwater resources.

In treating sewage water, there seems to be a number of techniques for decontamination. For eliminating pharmaceutically active substances, reverse osmosis (RO) and nano-filtration (NF) are the effective methods. Furthermore, before even being released into freshwater resources, the re-circulated stream containing high level contaminants must be eliminated (Simon *et al.*, 2009). These chemicals have been successfully removed using advanced oxidation processes (AOPs) such as ultraviolet (UV), semiconductor photo catalysis, Fenton and ozonation (Klavarioti *et al.*, 2009). As a result, AOPs have a great deal of capability for decomposing such compounds in sewage water. $LaNiO_3$ photo-catalysts has

gotten the greatest recognition because of their enhanced pursuit, thermal, chemical and photo-erosion tolerance, inexpensive, and eco-friendly (Yang *et al.*, 2011; Dzinun *et al.*, 2019). Even so, anatase $LaNiO_3$ with a broad band gap primarily accumulates gamma light (400 nm), that reports for 5–8% of solar energy and moreover gives rise to non-metals or metals being on condition that with visible light without damage of gamma action, extending the operational span and increasing productivity (Lin *et al.*, 2013). The replacement Sr doped $LaNiO_3$ is the most efficient among some of the non-metal doped-$LaNiO_3$, because of the bonding force amid the N 2p state and the O 2p state, therefore developing band-gap and shrinking Sr doped $LaNiO_3$ was capable in absorbing the light waves (Asahi *et al.*, 2001).

Molinari and his co-workers (Molinari *et al.*, 2002) were the first to create a hybrid method, which integrates membranes with catalysts. For the first time, a hybrid method was used to remove organic contaminants. Membrane serves as a barrier not just for molecule partition but also for catalyst isolation in this method. Photocatalytic membrane reactors (PMRs) can also conserve energy and minimize the complexity of an establishment (Molinari *et al.*, 2002; Mozia *et al.*, 2009). The PMR has also been used in treatment processes of sewage water (Hu *et al.*, 2019; Ly *et al.*, 2018), as well as to remove bacteria like *Aspergillus fumigatus* (Oliveira *et al.*, 2020) and medications like oxytetracycline (Espíndola *et al.*, 2019). Submerged photo-catalytic membrane reactor (SPMR) is a form of PMR with cheap setting costs, reduced energy consumption, and ease of management (Patsios *et al.*, 2013). The downsides of photo-catalytic immobilised in or above membrane, including a minor ratio of area-to-volume and lowered gamma light application efficacy (Patsios *et al.*, 2013; Mozia, 2010), as well as the loss and prolonged usage of catalyst particles in assembly lines, can be determined with SMPR (Patsios *et al.*, 2013; Chong *et al.*, 2010).

As per the knowledge of authors there were not many studies reported on Sr doped membranes on wastewater treatment especially on apocynin degradation. SPMRs with suspending and immobilised Sr-$LaNiO_3$ were examined for ACN elimination in continuous flow settings under gamma irradiation utilizing two photo-catalytic methods either with or without H_2O_2. For high effluent quality, RO membranes were paired through the SPMR after ceramic microfiltration membrane in the constant cycle. The levels of ACN, RO and total organic carbon in the MF filtrate was confirmed.

2. Methods and materials

2.1. Preparation of Sr-doped $LaNiO_3$

All the experimental reagents were analytical grade. A typical synthesis procedure was as follows: 0.9 mM of La $(NO_3)_3{\cdot}6H_2O$, 0.2 mM of Sr $(NO_3)_2$, and 2 mM of Ni $(NO_3)_2{\cdot}6H_2O$ were dissolved in 30 mL of N, N-Dimethylformamide and magnetically stirred for 4 h. Thereafter, 0.65 g of polyvinylpyrrolidone was added to the mixed to get a homogeneous solution by magnetically stirring it for 1.5 h. Subsequently, the homogeneous solution was heated under continuous stirring until the gel was formed. Then, the obtained gel was transferred to the crucible and placed in a muffle furnace for heating treatment at 730 °C for 2 h at a heating rate of 10 °C/min. The final synthesized product was nomenclatured as $La_{0.9}Sr_{0.1}NiO_3$-δ nanomaterials. Figure 1 illustrated the chemical structure of apocynin (ACN).

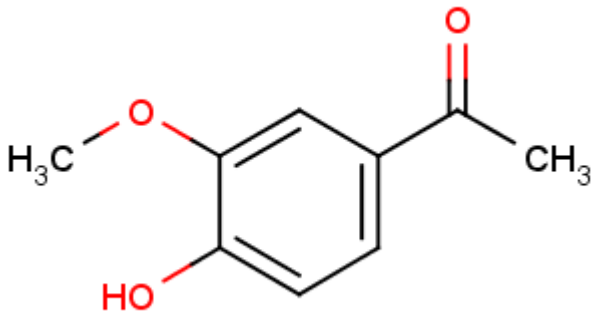

Figure 1. Chemical structure of apocynin (ACN)

2.2. Sr-$LaNiO_3$ immobilization on MF ceramic membrane

The overall surface of the MF membrane was 0.0150 m^2. To eliminate contaminants, the membrane area was rinsed numerous times with ethanol and desiccated at room temperature. In a mixer, 1.2 g Sr-$LaNiO_3$ particulates were added to 3.4 L of a sodium dioctyl sulfosuccinate solution (1.28 %), sonicated for 1.2 h to make the Sr-$LaNiO_3$ catalyst mixture. The MF membrane was gently immersed into the mixture, held in place for 2 min, and then steadily removed from the mixture. Lastly, the MF membranes were desiccated at 105°C in a kiln before being warmed to 550°C in a furnace at a heating rate of 10°C/min for 1.2 h. This technique was continued till the coating was spread to the appropriate thickness (Ciston *et al.*, 2006).

2.3. Experimental setup

During investigations on synthetic ACN-treated effluent water, SPMRs with suspended and immobilised Sr-doped $LaNiO_3$ on the ceramic membrane with observable illumination was utilized. It was also looked at combining H_2O_2 with the photo-catalytic method. The SPMR has a cylindrical photo-reactor container with a ceramic MF membrane embedded in the reactor's core and a conduit connecting it to a suction pump. A stainless-steel cylindrical photo-reactor tank with an operating capacity of 2.5 L was installed in a compartment. Around the exterior of the reactor, gamma source was mounted. A magnetic stirrer was used to guarantee that the ACN monomers and catalyst dispersion were homogeneous. The O_2 was transported through a canal suppressed below the MF membrane's base. There were batch and continuous procedures used.

For the batch tests, an SPMR with suspended and immobilised Sr-$LaNiO_3$ was employed for 200 min to examine the ACN extraction efficacy under Vis/ Sr-$LaNiO_3$ and Vis/ Sr-$LaNiO_3$ / H_2O_2 procedures. The impacts of the

initial Sr-$LaNiO_3$ levels on the extraction efficacy were also looked at. The SPMR was connected to a RO membrane for constant circumstances. Outside the photo-catalytic reactor, the RO membrane was linked to the yield of pumping system. The Vis/ Sr-$LaNiO_3$ and Vis/ Sr-$LaNiO_3$ / H_2O_2 procedures were used for 72 h on SPMRs with suspended and immobilised Sr-$LaNiO_3$. Through a hose, a feed tank was linked to the photo reactor. A regulating float was utilized to regulate the operating capacity of the photo-catalytic reactor, and a lever was employed to manage the RO membrane's discharge rate of flow. The RO permeate was mechanically reused into the reaction vessel. In this work, alternating performances of the SPMR units with a configuration of 8 min of operation (ON) and 2 min of halt were used to prevent membrane fouling (OFF). The MF and RO membranes' wastewater grade and pervade deadline were examined. Figure 2 illustrated the schematic representation of experimental setup.

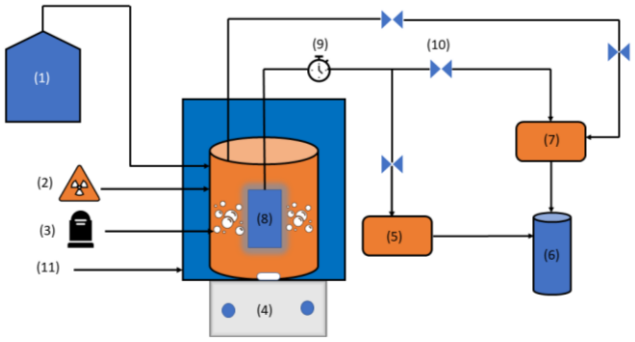

Figure 2. Schematic representation of experimental setup. 1) Feed tank, 2) Gamma irradiation, 3) Oxygen supply, 4) Magnetic stirrer, 5) Micro filtration (MF) permeates, 6) Reverse osmosis permeate, 7) Reverse osmosis membrane, 8) MF membrane, 9) Timer, 10) Suction pump, 11) Chamber.

2.4. Analytical methods

At a wavelength of 300 nm, a UV-Vis spectrophotometer has been employed to assess the ACN contents. For the TOC assessment, a TOC analyzer model was used. Potassium phthalate norms were used to tune the instruments.

3. Result and discussion

3.1. Batch photo-catalytic reactor

Batch experiments were conducted for each setting to assess ACN elimination through photocatalysis; RO membrane, MF membrane with and without immobilised Sr-$LaNiO_3$ on the exterior layer, and also H_2O_2. 60 mg/L ACN, pH 7, 2 g/L Sr-$LaNiO_3$ infusion into SMPR with dispersion, and 2 g Sr-$LaNiO_3$ deposited on MF membrane surfaces were used as the laboratory parameters. All of the trials were completed in 180 min. The research found that MF membrane, MF membrane coated Sr-$LaNiO_3$, and H_2O_2 alone elimination relatively little ACN at high concentrations (60 mg/L). The elimination of ACN by RO membrane has been estimated to be as high as 98%, showing that RO membrane has a great capability to exclude ACN molecule. The findings were in line with prior research, which shows that RO membranes may exclude negatively charged ACN molecules up to 96% (Kimura *et al.*, 2003). The difference in MF and RO extraction efficiency might be attributed to their pore diameters or molecular weight cut off (MWCO) (Verliefde *et al.*, 2007). For instance, MF membrane pore diameters vary from 0.2 to 5.4 m or a MWCO larger than 1,500 kDalton, whereas RO membrane pore sizes vary from 0.0002 to 0.002 m (MWCO less than 110 Dalton). Meanwhile, ACN has a molecular weight of 300 (g/mol). ACN with such a molecular weight can easily flow through the MF membrane, but it will be denied by the RO membrane. In comparison to MF membranes sans coated Sr-$LaNiO_3$ on the surface, MF membranes with Sr-$LaNiO_3$ immobilisation on the surface demonstrated somewhat greater ACN elimination. The discovery might be the cause of ACN monomers being deposited on the membrane surface by Sr-$LaNiO_3$ nanoparticles. Figure 3 illustrated the SEM micrographs of synthesized Sr-doped $LaNiO_3$.

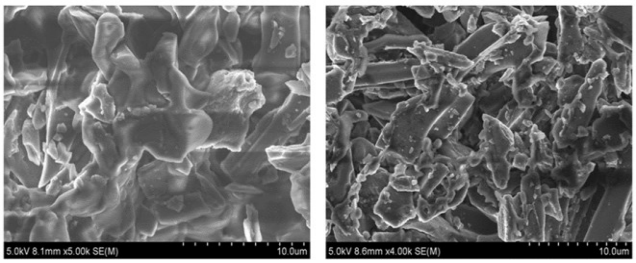

Figure 3. SEM micrographs of synthesized Sr-doped $LaNiO_3$

3.1.1. Impacts of Sr-doped $LaNiO_3$ accumulation in refinement process

In the batch settings, the influence of the starting Sr-$LaNiO_3$ level on the ACN extraction efficacy by the SPMR containing dispersed Sr-$LaNiO_3$ under Vis/ Sr-$LaNiO_3$ and Vis/ Sr-$LaNiO_3$ / H_2O_2 procedures is shown in Figure 4. The ACN remaining in reactor (ACN level) measured by the SPMR with suspended Sr-$LaNiO_3$ during the photo-catalytic activity (Vis/N-TiO_2 procedure) is shown in Figure 4a. For whatever starting Sr-$LaNiO_3$ level, ACN elimination did not achieve 100% after 200 min. With 0.6 g/L Sr-$LaNiO_3$, the lowest ACN and TOC elimination efficacy were achieved. At low catalytic dosages, there aren't enough photo-catalytic active sites in $LaNiO_3$, leading in a slow decomposition pace (Chin *et al.*, 2007).

The ACN and TOC elimination efficiencies were lowered when the initial Sr-$LaNiO_3$ level was increased to 2 g/L compared to 1 and 1.5 g/L. Because the probing photon flux adsorbs to the catalyst surface when the catalyst dose is increased beyond saturation, the deterioration process may be slowed (Wang *et al.*, 2013). Furthermore, a high catalyst dose causes agglomeration of the catalyst, leading to reduced surface area (Shon *et al.*, 2008). With a starting Sr-$LaNiO_3$ level of 0.5 g/L, the highest ACN extraction efficacy was 54%. The deterioration rate rises at necessary catalyst doses since it avoids unwanted surplus catalyst and ensures full photon adsorption for effective photo-mineralization (Reza *et al.*, 2017). Because of the impacts on the catalyst surface and absorption of the photon flux on the exterior area of the catalyst, the catalyst dose has a positive or negative influence the photo-degradation rates in overall. The ACN elimination effectiveness using the

photo-catalytic method combined with H_2O_2 is shown in Figure 4b. The best initial Sr-$LaNiO_3$ level for ACN elimination using this procedure was 2 g/L, and the smallest ACN elimination appeared at 0.5 g/L, implying that the elimination efficacy for both photo-catalytic activity, with (Vis/ Sr-$LaNiO_3$ / H_2O_2) and without (Vis/ Sr-$LaNiO_3$ procedure), was maximized with the same initial Sr-$LaNiO_3$ level. Furthermore, as contrasted to exclusively photo-catalytic activity under visible irradiation, combining H_2O_2 with the photo-catalytic activity improved ACN and TOC elimination. H_2O_2 may readily interact with $LaNiO_3$ electrons to create hydroxyl radicals when combined with the photo-catalytic activity (Velegraki *et al.*, 2006). Furthermore, the interaction involving H_2O_2 and the oxygen species generates higher hydroxyl radicals in the photo-catalytic activity (Irmak *et al.*, 2004). Additionally, the deposited H_2O_2 on the $LaNiO_3$ surface forms proxy compounds with the Sr ions, increasing the adsorption capability of $LaNiO_3$ when exposed to visible light (Zou *et al.*, 2011). The use of H_2O_2 in conjunction with the photo-catalytic method improves the elimination of ACN and TOC.

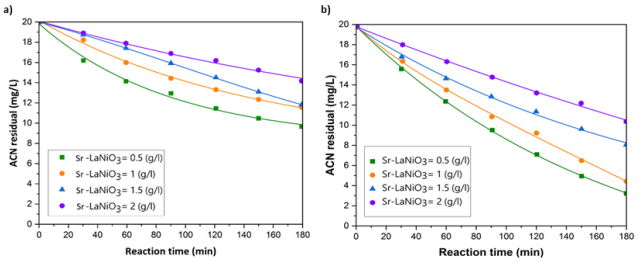

Figure 4. The impact of Sr-$LaNiO_3$ feeding on ACN deterioration by SPMR with stranded Sr-$LaNiO_3$; (a) Vis/ Sr-$LaNiO_3$ procedure, (b) Vis/ Sr-$LaNiO_3$ / H_2O_2 procedure. Levels of Sr-$LaNiO_3$ of 0.4, 1.0, 1.5, and 2.0 g/L were used in the experiments. [ACN] = 25 mg/L, observable light range = 300 W, and [H_2O_2] = 20 mM. pH = 7, [ACN] = 20 mg/L, observable light range = 300 W, and [H_2O_2] = 20 mM.

3.2. Regular parameters

3.2.1. Permeate quality

For SPMR with suspended and immobilised Sr-$LaNiO_3$, the longstanding constant operation capabilities of the Vis/ Sr-$LaNiO_3$ and Vis/ Sr-$LaNiO_3$ / H_2O_2 procedures were investigated. The Sr-$LaNiO_3$ loading was 2 g/L, the solution pH was 7, and the input ACN content was 25 mg/L. The RO permeate flow rate was maintained at 2.6 L/h, which corresponded to a hydraulic retention time (HRT) of 5 h. The ACN mixture was constantly delivered from the feed tank into the photo reactor. In the Vis/ Sr-$LaNiO_3$ / H_2O_2 procedure, H_2O_2 was combined with the ACN solution in the storage tank. The SPMR entity used sporadic membrane filtration and were monitored by a timer that interchanged amid 6 min of work (ON) and 2 min of stop (OFF). The long duration trials lasted for 72 h. At periodic times, samples taken from the MF and RO penetrates to determine the remaining ACN and TOC in the solution. To manage the SPMR's HRT, the RO permeate flow was monitored for 5 h. After 5 h, the MF permeate flow was determined using the MF membrane outflow. Under photo-catalytic operations with and without H_2O_2, the ACN levels in the MF and RO penetrates in the SPMR with suspended and immobilised Sr-$LaNiO_3$ are shown in Figure 5. The findings demonstrate that during the initial 3 h, the ACN levels in MF permeates (ACN level in the photo reactor) tended to decrease for all operations. They also grew steadily after 4 h till the completion of the experiment Throughout the study, the ACN contents in the RO filtrate (effluent) were constant. The ACN molecules flowing via MF membrane were restored to the SPMR via RO refusal as the ACN level in the photo-catalytic reactor increased. The SPMR treatment capability was overloaded due to rising ACN levels in the photo-catalytic reactor. As an outcome, the levels of ACN in the photo reactor rose. The ACN levels in the SPMR with immobilised Sr-$LaNiO_3$ were greater than those with suspended Sr-$LaNiO_3$ during the photo-catalytic process (Vis/ Sr-$LaNiO_3$). This implies that in the constant cycle, SPMRs with the immobilised Sr-$LaNiO_3$ catalyst had a poorer ACN extraction efficacy than SPMRs with suspended Sr-$LaNiO_3$. In comparison to the procedures without irradiation, combining H_2O_2 with the photo-catalytic activity improved ACN elimination under observable illumination for both SPMR entities with suspended and immobilised Sr-$LaNiO_3$. The ACN elimination efficacy possibilities of the numerous SPMR samples with various photo-catalytic activity were in the following manner: SPMR with dispersed Sr-$LaNiO_3$ under the Vis/ Sr-$LaNiO_3$ / H_2O_2 process > SPMR with immobilised Sr-$LaNiO_3$ under the Vis/ Sr-$LaNiO_3$ / H_2O_2 procedures > SPMR with dispersed Sr-$LaNiO_3$ under the Vis/ Sr-$LaNiO_3$ procedures> SPMR with immobilised Sr-$LaNiO_3$ under the Vis/ Sr-$LaNiO_3$ procedures.

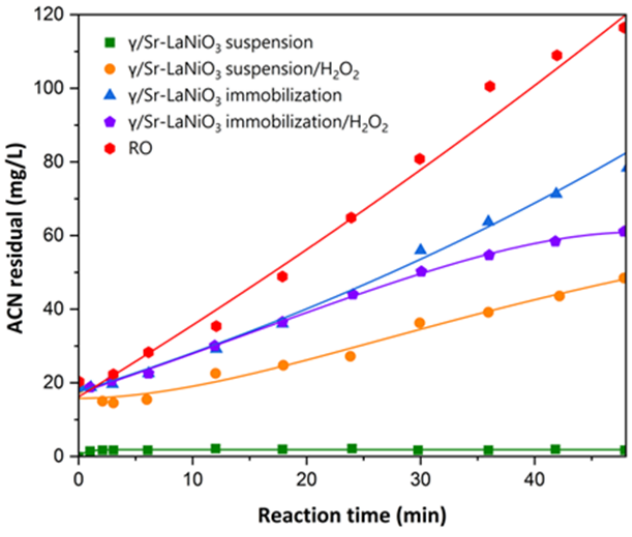

Figure 5. Periodic change of ACN leftover for 4 SPMR systems with RO membrane under long-term settings. Circumstances of the test: pH = 7; starting ACN = 25 mg/L; Sr-$LaNiO_3$ loading =2g/L for suspended Sr-$LaNiO_3$; H_2O_2 = 20 mM for Vis/ Sr-$LaNiO_3$ / H_2O_2 process; intermittent membrane filtration: 10 minutes ON, 2 minutes OFF.

The majority of ACN molecules went through the MF membrane, whereas the RO membrane discarded them more frequently. Throughout the operating duration, the ACN contents in the RO filtrate for the SPMRs with

suspended or immobilised Sr-$LaNiO_3$ and photo-catalytic procedures with or without H_2O_2 were less than 3 mg/L. The photo-catalytic membrane reactor, which integrated the MF membrane with an RO membrane in an PMR reduced RO membrane contamination as well as enhanced wastewater standard. Furthermore, the mixture resulted in a large rise in ACN levels in the photo reactors, causing an overflow in the SPMR system's processing capability.

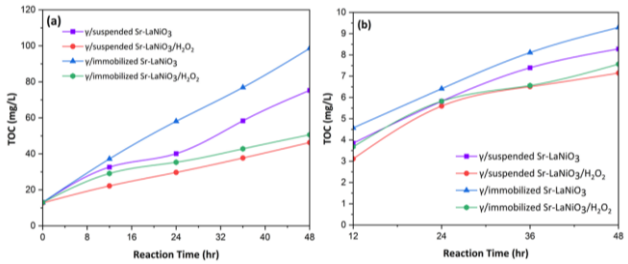

Figure 6. ACN mineralization throughout longstanding circumstances, (a) TOC of MF permeates, (b) TOC of RO permeates. pH = 7; starting ACN = 30 mg/L; Sr-$LaNiO_3$ loading =2 g/L for suspended Sr-$LaNiO_3$; H_2O_2 = 20; periodic membrane filtration of 6 min ON and 2 min OFF.

The ACN discharges and the percent of elimination by the RO membrane are shown in Table 1. The proportion of ACN discarded by the RO membrane was around 97%, which corresponded to the findings, which showed that RO membranes may exclude negatively charged ACN up to 97% (20). Membrane characteristics, flow rate, and operation circumstances are all parameters that influence RO membrane denial (Bellona and Drewes, 2005). Furthermore, 3 processes might alter the solute's filtration by the RO membrane: physicochemical interactions between the solute, solvent and size confinement (sieving, steric effect) and membrane and charge confinement (electrical, Donnan) (Radjenović *et al.*, 2008) ACN has a pKa of 4.15, making it negatively charged, which lowers hydrophobicity and promotes solubility when pH = 6.5. As a result, a significant negative charge on the RO membrane, according to Donnan's theory, effectively denies the ACN, inhibiting diffusion and adsorption across the membrane. The often-employed measure for predicting filtering procedure's elimination effectiveness is molecular weight (21). ACN has a molecular weight of 300 g/mol and dimensions of 1.15× 0.95× 0.50 nm, correspondingly. An RO membrane can eliminate molecules with molecular weights greater than 250 g/mol, implying that ACN, with a molecular weight of 300 g/mol, may be processed (Lipp *et al.*, 2010).

At the time of 72 h of photo-catalytic oxidation, TOC concentration is eliminated by the MF (Figure 6a) and RO permeates (Figure 6b). The TOCs content in the photo-reactors and wastewater rose at the time of the reaction period for both SPMR structures and procedures, according to the findings. In the photo-reactor, the SPMR with immobilised Sr-$LaNiO_3$ under the Vis/ Sr-$LaNiO_3$ procedures showed the quickest rise in TOC level. The SPMR with suspended Sr-$LaNiO_3$ under the Vis/ Sr-$LaNiO_3$/ H_2O_2 procedure had the least rise in TOC content (Figure 6a). The restoration of ACN monomers and compounds to the reactor via RO rebuff causes a rise in TOC levels in the photo-reactor. During the reaction period, the TOC contents in the wastewaters also increases (Figure 6b). The lower molecular weight cut-off (MWCO) of the intervening products that may permeate via the pores of the membrane is connected to the increasing TOC levels in the RO penetrates (wastewater). These findings show that the RO membrane was critical in refusing not only the ACN molecules, but also their yields, and redirecting them to the photo-catalytic reactor for addition of minerals. The mixture of the RO membrane and the SPMR units led to enhanced wastewater standard and higher ACN breakdown into lower molecular weight compounds.

Table 1. ACN elimination through Reverse Osmosis membrane rebuff

SPMR process MF permeate	MF permeate = Reverse Osmosis feed (milligram per litre)	Reverse Osmosis permeate (milligram per litre)	Reverse Osmosis rebuff (%)
Vis/suspended Sr-$LaNiO_3$	41.23±20.23	1.55±0.53	96.34±2.76
Vis/suspended Sr-$LaNiO_3$ / H_2O_2	27.23±11.34	1.45±0.32	95.23±2.45
Vis/immobilized Sr-$LaNiO_3$	57.12±33.56	1.99±0.34	96.12±3.01
Vis/immobilized Sr-$LaNiO_3$ / H_2O_2	37.23±16.00	1.45±0.23	96.01±2.65

3.2.2. Permeate flux of MF and RO membrane

The penetrate fluxes across the MF and RO membranes was examined for long working term by regulating the proportion of flow, the MF and RO permeates later 5 h. An RO permeates proportion of flow were monitored and controlled with a valve to keep the RO proportion at a constant flow rate of 2 L/h. With the multiple methods (Vis/ Sr-$LaNiO_3$ and Vis/ Sr-$LaNiO_3$ / H_2O_2), the MF permeate fluxes of the SPMR entities change. The data indicates that the MF permeate flow of the SPMR with suspended Sr-$LaNiO_3$ were lowered rapidly first, by way of a little drop later 30 h, but the MF permeate flux of the SPMR with immobilised Sr-$LaNiO_3$ were stable first, then fell significantly after 9h. Under the Vis/ Sr-$LaNiO_3$ method, the SPMR's MF permeate flux reduced faster than under the Vis/ Sr-$LaNiO_3$ / H_2O_2 operation. A decline in permeate flux, which can be caused by pore blockage, the creation of a cake layer on the surface of the membrane, smaller apertures, or foulant absorption of pores of the membrane, indicates membrane besmirching (Zhang *et al.*, 2015). The initial decrease in MF permeate flow in the SPMR with scattered Sr-$LaNiO_3$ was due to nanoparticles of Sr-$LaNiO_3$ connected to the exterior layer of the membrane, whereas the flux in the SPMR with fixed Sr-$LaNiO_3$ held steady. When compared to disperse $LaNiO_3$, there were several benefits to immobilised $LaNiO_3$ on the membrane, including no need to remove and reuse

catalysts, less membrane fouling, and improved wastewater quality owing to smaller membrane pores (Zhang *et al.*, 2009). Nevertheless, there are certain drawbacks, including a poor catalyst area ratio, the inability to alter catalyst concentration, and the need for membrane renewal when the catalyst on the membrane is depleted. Whereas a $LaNiO_3$ layer forms on the membrane, $LaNiO_3$ nanoparticles can lead to the MF permeate flow to decrease (Shon *et al.*, 2008). The permeate flow is limited by elevating the $LaNiO_3$ concentration in the reactor. The naked eye was used to examine the surface of the MF membrane. The cake layer generated upon the MF membrane of the SPMR with dispersed Sr-$LaNiO_3$ under Vis/ Sr-$LaNiO_3$ was denser when compared to any other reactors, after 72 h of operation. Permeation was diminished because the combination of ACN and Sr-$LaNiO_3$ particles formed on the membrane had already become denser (Figure 7). The cake layer of $LaNiO_3$ with the organic component become denser at high organic levels (Wang *et al.*, 2013).

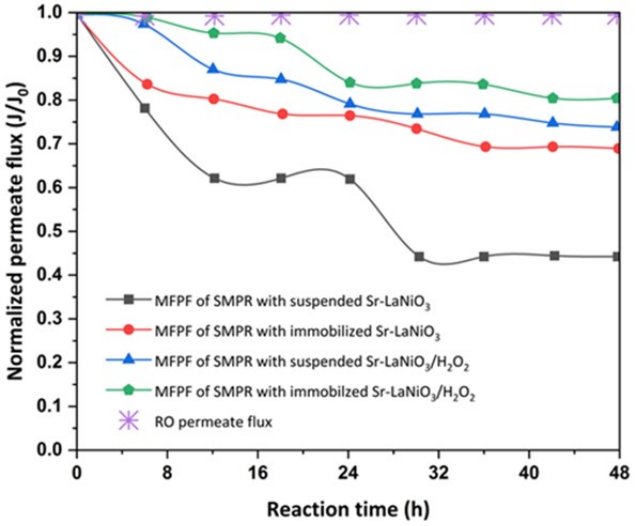

Figure 7. Changes in MF and RO permeate flow in constant settings. Initial ACN = 30 mg/L, Sr-$LaNiO_3$ loading = 2 g/L for suspended Sr-$LaNiO_3$; H_2O_2 = 30 mM for Vis/ Sr-$LaNiO_3$ / H_2O_2 procedure; pH = 7; and sporadic membrane filtration of 6 min ON and 2 min OFF.

4. Conclusion

The efficacy of ACN exclusion in the photo-catalytic procedure with and without H_2O_2 was revised by the initial Sr-$LaNiO_3$ concentrations. Under visible irradiation, the greatest photo-catalytic ACN elimination efficacy was found at a Sr-$LaNiO_3$ level of 2 g/L. The use of H_2O_2 in conjunction with the photo-catalytic activity increased the effectiveness of ACN elimination. When the SPMRs with suspended and immobilised Sr-$LaNiO_3$ were compared, it was discovered that the SPMR with suspended catalyst had a higher ACN extraction efficacy because the Sr-$LaNiO_3$ particles increased ACN elimination. SPMRs with suspended and immobilised Sr-$LaNiO_3$ have both benefits and drawbacks. By raising the Sr-$LaNiO_3$ dose, the response proportion in the SPMR with dispersed Sr-$LaNiO_3$ may be increased. The SPMR with immobilised Sr-$LaNiO_3$ particle, on the other hand, exhibited less membrane fouling when compared to SPMR with dispersed Sr-$LaNiO_3$ molecules. When H_2O_2 was combined with the photo-catalytic activity, membrane fouling was reduced compared to when the photo-catalytic method was used separately. The pairing of the RO membrane and the SPMR produced high-quality wastewater. Nevertheless, since ACN and its by-products were restored to the photo reactor via RO repudiation, the ACN and TOC levels in the photo reactor raised. The Sr-$LaNiO_3$ particles combined with the organic compounds formed a cake layer on the MF membrane surface, which were principally capable in lowering MF permeate flow of the SPMR.

Conflicts of interest

No Conflict of Interest

References

Acero J.L., Benítez F.J., Leal I., Real F.J. (2005 Aug 1). Removal of phenolic compounds in water by ultrafiltration membrane treatments. *Journal of Environmental Science and Health, Part A [Internet]*, **40**(8), 1585–1603. Available from: https://doi.org/10.1081/ESE-200060651

Asahi R., Morikawa T., Ohwaki T., Aoki K., and Taga Y. (2001). Visible-light photocatalysis in nitrogen-doped titanium oxides. *Science (80-)*, **293**(5528), 269–271.

Bellona C., and Drewes J.E. (2005). The role of membrane surface charge and solute physico-chemical properties in the rejection of organic acids by NF membranes. *Journal of Membrane Science*, **249**(1–2), 227–234.

Chin S.S., Lim T.M., Chiang K., Fane A.G. (2007). Factors affecting the performance of a low-pressure submerged membrane photocatalytic reactor. *Chemical Engineering Journal*, **130**(1), 53–63.

Chong M.N., Jin B., Chow C.W.K., and Saint C. (2010). Recent developments in photocatalytic water treatment technology: a review. *Water Research*, **44**(10), 2997–3027.

Ciston S., Chen L., Li G., Hausner M., Lueptow R.M., and Gray K.A. (2006). Effects of TiO2 nanostructure and various ceramic supports in photocatalytic membranes for water treatment. In: 2006 AIChE Annual Meeting San Francisco, CA. 2006.

Dzinun H., Othman M.H.D., and Ismail A.F. (2019). Photocatalytic performance of TiO2/Clinoptilolite: Comparison study in suspension and hybrid photocatalytic membrane reactor. *Chemosphere*, **228**, 241–248.

Espíndola J.C., Cristóvão R.O., Mendes A., Boaventura R.A.R., and Vilar V.J.P. (2019). Photocatalytic membrane reactor performance towards oxytetracycline removal from synthetic and real matrices: Suspended vs immobilized TiO2-P25. *Chemical Engineering Journal*, **378**, 122114.

Hu C., Wang M-S., Chen C-H., Chen Y-R., Huang P-H., and Tung K-L. (2019). Phosphorus-doped g-C3N4 integrated photocatalytic membrane reactor for wastewater treatment. *Journal of Membrane Science*, **580**, 1–11.

Irmak S., Kusvuran E., and Erbatur O. (2004). Degradation of 4-chloro-2-methylphenol in aqueous solution by UV irradiation in the presence of titanium dioxide. *Applied Catalysis B-Environmental*, **54**(2), 85–91.

Kimura K., Amy G., Drewes J.E., Heberer T., Kim T-U., and Watanabe Y. (2003). Rejection of organic micropollutants (disinfection by-products, endocrine disrupting compounds,

and pharmaceutically active compounds) by NF/RO membranes. *Journal of Membrane Science*, **227**(1–2), 113–121.

Klavarioti M., Mantzavinos D., and Kassinos D. (2009). Removal of residual pharmaceuticals from aqueous systems by advanced oxidation processes. *Environment International*, **35**(2), 402–17.

Lin Y-T., Weng C-H., Lin Y-H., Shiesh C-C., and Chen F-Y. (2013). Effect of C content and calcination temperature on the photocatalytic activity of C-doped TiO2 catalyst. *Separation and Purification Technology,* **116**, 114–123.

Lipp P., Sacher F., and Baldauf G. (2010). Removal of organic micro-pollutants during drinking water treatment by nanofiltration and reverse osmosis. *Desalin Water Treatment*, **13**(1–3), 226–237.

Ly Q.V., Kim H-C., and Hur J. (2018). Tracking fluorescent dissolved organic matter in hybrid ultrafiltration systems with TiO2/UV oxidation via EEM-PARAFAC. *Journal of Membrane Science*, **549**, 275–282.

Madureira J., Pimenta A.I., Popescu L., Besleaga A., Dias M.I., Santos P.M.P., *et al.* (2017). Effects of gamma radiation on cork wastewater: Antioxidant activity and toxicity. *Chemosphere [Internet]*, **169**, 139–145. Available from: https://www.sciencedirect.com/science/article/pii/S0045653516315995

Molinari R., Palmisano L., Drioli E., and Schiavello M. (2002). Studies on various reactor configurations for coupling photocatalysis and membrane processes in water purification. *Journal of Membrane Science*, **206**(1–2):399–415.

Mozia S. (2010). Photocatalytic membrane reactors (PMRs) in water and wastewater treatment. A review. *Separation and Purification Technology*, **73**(2), 71–91.

Mozia S., Morawski A.W., Toyoda M., and Tsumura T. (2009). Effect of process parameters on photodegradation of Acid Yellow 36 in a hybrid photocatalysis–membrane distillation system. *Chemical Engineering Journal*, **150**(1), 152–159.

Oliveira B.R., Sanches S., Huertas R.M., Crespo M.T.B., and Pereira V.J. (2020). Treatment of a real water matrix inoculated with Aspergillus fumigatus using a photocatalytic membrane reactor. *Journal of Membrane Science*, **598**, 117788.

Patsios S.I., Sarasidis V.C., and Karabelas A.J. (2013). A hybrid photocatalysis–ultrafiltration continuous process for humic acids degradation. *Separation and Purification Technology*. 2013;104:333–41.

Radjenović J., Petrović M., Ventura F., and Barceló D. (2008). Rejection of pharmaceuticals in nanofiltration and reverse osmosis membrane drinking water treatment. *Water Research*, **42**(14), 3601–3610.

Reza K.M., Kurny A.S.W., and Gulshan F. (2017). Parameters affecting the photocatalytic degradation of dyes using TiO_2: a review. *Applied Water Science*, **7**(4), 1569–1578.

Sevimli M.F. (2005 Feb 1). Post-treatment of pulp and paper industry wastewater by advanced oxidation processes. *Ozone: Science and Engineering [Internet]*, **27**(1), 37–43. Available from: https://doi.org/10.1080/01919510590908968

Shon H.K., Phuntsho S., and Vigneswaran S. (2008). Effect of photocatalysis on the membrane hybrid system for wastewater treatment. *Desalination*, **225**(1–3):235–248.

Simon A., Nghiem L.D., Le-Clech P., Khan S.J., Drewes J.E. (2009). Effects of membrane degradation on the removal of pharmaceutically active compounds (PhACs) by NF/RO filtration processes. *Journal of Membrane Science*, **340**(1–2):16–25.

Velegraki T., Poulios I., Charalabaki M., Kalogerakis N., Samaras P., and Mantzavinos D. (2006). Photocatalytic and sonolytic oxidation of acid orange 7 in aqueous solution. *Applied Catalysis B: Environmental*, **62**(1–2), 159–168.

Verliefde A., Cornelissen E., Amy G., Van der Bruggen B., Van Dijk H. (2007). Priority organic micropollutants in water sources in Flanders and the Netherlands and assessment of removal possibilities with nanofiltration. *Environmental Pollution*, **146**(1), 281–289.

Wang P., Fane A.G., and Lim T-T. (2013). Evaluation of a submerged membrane vis-LED photoreactor (sMPR) for carbamazepine degradation and TiO2 separation. *Chemical Engineering Journal*, **215**, 240–251.

Yang S., Gu J-S., Yu H-Y., Zhou J., Li S-F., Wu X-M., *et al.* (2011). Polypropylene membrane surface modification by RAFT grafting polymerization and TiO2 photocatalysts immobilization for phenol decomposition in a photocatalytic membrane reactor. *Separation and Purification Technology*, **83**, 157–165.

Zhang W., Liang W., Huang G., Wei J., Ding L., and Jaffrin M.Y. (2015). Studies of membrane fouling mechanisms involved in the micellar-enhanced ultrafiltration using blocking models. *RSC Advances*, **5**(60), 48484–48491.

Zhang X., Pan J.H., Du A.J., Fu W., Sun D.D., Leckie J.O. (2009). Combination of one-dimensional TiO2 nanowire photocatalytic oxidation with microfiltration for water treatment. *Water Research*, **43**(5), 1179–1186.

Zou J., and Gao J. (2011). H2O2-sensitized TiO2/SiO2 composites with high photocatalytic activity under visible irradiation. *Journal of Hazardous Materials*, **185**(2–3):710–716.